Electronic Supplementary Material (ESI) for Journal of Materials Chemistry A.

Mesoporous calcium oxide-silica and magnesium oxide-silica composites for CO_2 capture at ambient and elevated temperatures

Chamila Gunathilake and Mietek Jaroniec*

Department of Chemistry and Biochemistry, Kent State University, Kent, Ohio 44242, USA
E-mail: jaroniec@kent.edu

Materials

Magnesium nitrate hexahydrate $Mg(NO_3)_2.6H_2O$ and calcium nitrate tetrahydrate $Ca(NO_3)_2.4H_2O$ were purchased from Acros Organic, New Jersey. Pluronic P123 ($EO_{20}PO_{70}EO_{20}$) triblock copolymer was donated by BASF Corporation, Florham Park, New Jersey. 95 % Ethanol and 36 % HCl, were purchased from Fisher Scientific, Pittsburgh, Pennsylvania. Tetraethylorthosilicate (TEOS) was purchased from Gelest Inc., Morrisville, Pennsylvania.$CaCO_3$ and $MgCO_3$ were purchased from Sigma-Aldrich St. Louis, MO.Deionized water (DW) was obtained using in house Ion pure Plus 150 Service Deionization ion-exchange purification system. All reagents were analytical grade and used without further purification.

Characterization

Characterization procedures provided below are analogous to those reported in [1-3]. Nitrogen adsorption isotherms were measured at -196 ^oC on an ASAP 2010 volumetric analyzer (Micromeritics, Inc., Norcross, GA). Prior to adsorption measurements, all samples were out gassed under vacuum at 110 ^oC for 2 h.

High resolution thermogravimetric measurements were recorded on TGA Q-500 analyzer (TA Instruments, Inc., New Castle, DE).Thermogravimetric (TG) profiles were recorded from 25 to 800 ^oC in flowing nitrogen with a heating rate of 10 ^oC / min using a high resolution mode. The weight of each sample was typically in 5-20 mg range. The TG profiles were used to obtain information about the extent of the template removal.

Transmission electron microscopy (TEM) images were obtained on a FEI Tecnai G2 F20 microscope. Prior to TEM analysis, the sample powders were dispersed in ethanol by moderate sonication at concentrations of ~5 wt. %. A Lacy carbon coated, 200-mesh, copper TEM grid was dipped into the sample suspension and then dried under vacuum at 80 ^oC for 12 h. SEM images were taken on a Hitachi S-2600N scanning electron microscope (1-30 kV) using solid state back scattered electron detector. The energy dispersive X-ray spectroscopy (EDX) data

were recorded by using an integrated scanning TEM (STEM) unit with attached EDAX spectrometer.

^{1}H-^{29}Si cross polarization (CP) MAS NMR spectra were recorded at 9.4 T using Bruker Avance (III) 400WB NMR spectrometer (Bruker Biospin Corporation, Billerica, MA, USA) with MAS triple resonance probe head using zirconia rotors 4 mm in diameter. Frequencies of ^{1}H-^{29}Si (CP) MAS NMR spectra were recorded at 79.49 MHz for ^{29}Si and 400.13 MHz for ^{1}H. The MAS rate was 5 KHz. ^{1}H $\pi/2$ pulse length was 4.5 μs and pulse delay 3.0 s. Two pulse phase modulated TPPM15 decoupling sequence was used during acquisition. The ^{29}Si chemical shifts were referenced to TMS (0 ppm).

Calculations

The protocol of analysis of adsorption data is analogous as in [1-3]. The Brunauer-Emmett-Teller specific surface areas (S_{BET}) were calculated from N_2 adsorption isotherms in the relative pressure range of 0.05-0.2 using a cross sectional area of 0.162 nm^2 per nitrogen molecule. The single-point pore volume (V_{sp}) was estimated from the amount adsorbed at a relative pressure of ~ 0.98. The pore size distributions (PSD) were calculated using adsorption branches of nitrogen adsorption-desorption isotherms by the improved KJS method calibrated for cylindrical pores [4]. The pore width (W_{max}) was obtained at the maximum of the PSD curve. The micropore volume (V_{mi}) was evaluated by integration of the PSD curve up to ~3 nm.

Isoelectric heat of adsorption.

The Clausius-Clapeyron relationship was employed to evaluate the isosteric heat of adsorption using the linear plots of ln (P/P^{o}) as a function of 1/T at constant values of the amount adsorbed a; symbols P, P_o, and T denote theequilibrium pressure, saturation vapor pressure, and temperature, respectively.

(1) Gunathilake, C.; Jaroniec, M. Mesoporous organosilica with amidoxime groups for CO_2 sorption. *Appl.Mater.Interfaces*. **2014**, 6, 13069–13078.

(2) Gunathilake, C.; Jaroniec, M., Mesoporous alumina-zirconia-organosilica composites for CO_2 capture at ambient and elevated temperatures. *J. Mater. Chem. A.* **2015**, 3, 2707-2716.

(3) Gunathilake, C.; Gorka, J.; Dai, S.; Jaroniec, M. Amidoxime modified mesoporous silica for Uranium adsorption under seawater conditions. *J. Mater. Chem. A.* **2015**, 3, 11650-11659.

(4) Kruk, M.; Jaroniec, M.; Sayari, A. Application of large pore MCM-41 molecular sieves to improve pore size analysis using nitrogen adsorption measurements. *Langmuir*, **1997**, 13, 6267-6273.

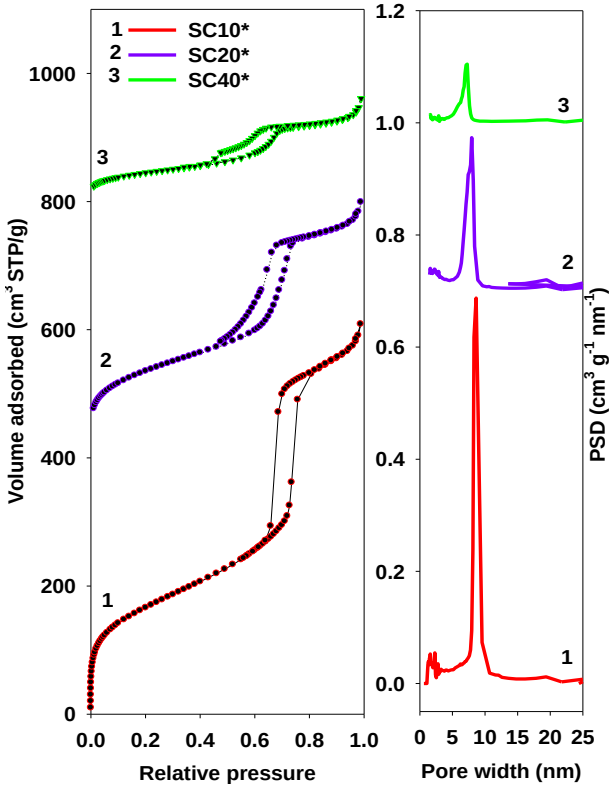

Figure S1. Nitrogen adsorption isotherms (left panel) and the corresponding PSD curves (right panel) for the SCX* samples studied; isotherms curves 2 and 3 are shifted by 500 and 800 cm^3 STP / g, respectively, in relation to curve 1, while the PSD curves 2 and 3 are shifted by 0.7 and 1.0 cm^3 g^{-1} nm^{-1}, respectively, in relation to curve 1.

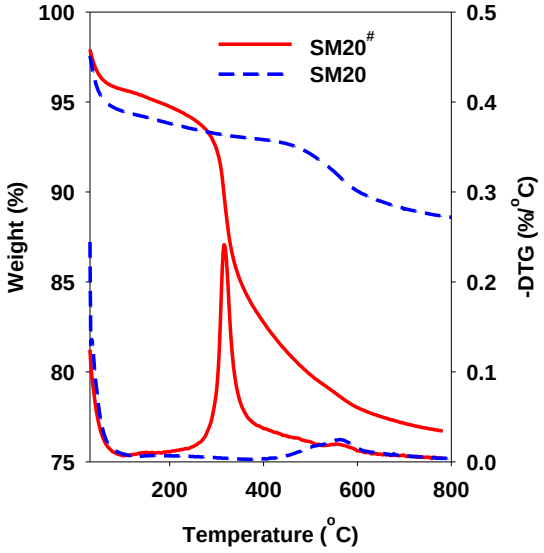

Figure S2. TG/DTG curves for the as-synthesized ($SM20^{\#}$) and thermally treated (SM20) samples.

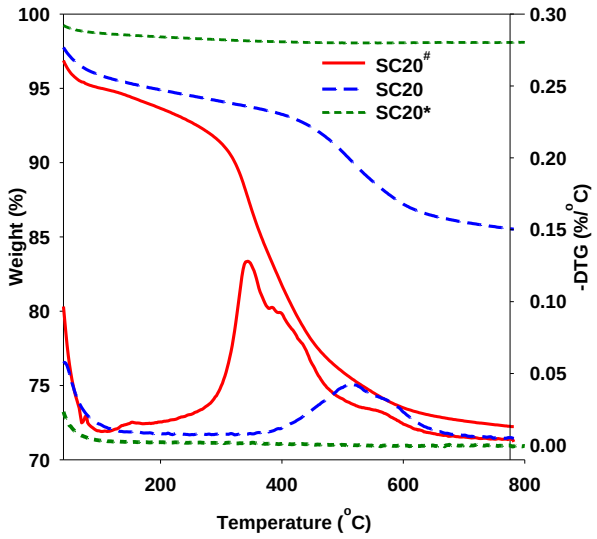

Figure S3.TG/DTG curves for the as-synthesized (#) and thermally treated (550 and 850 ^{o}C) SC20 samples.

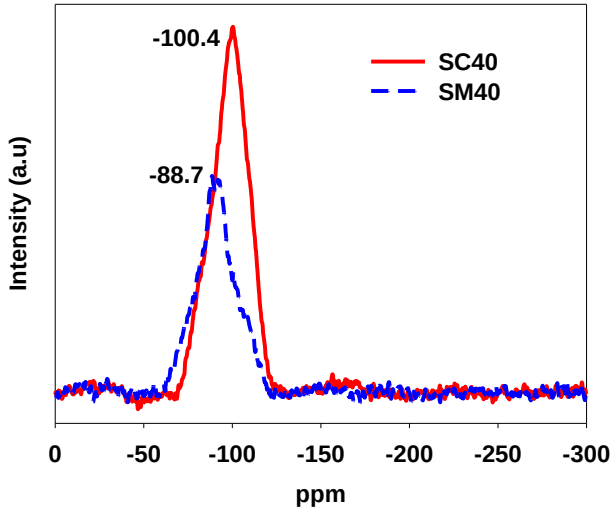

Figure S4.^{1}H-^{29}Si-MAS NMR spectra of the SC40 and SM40samples.

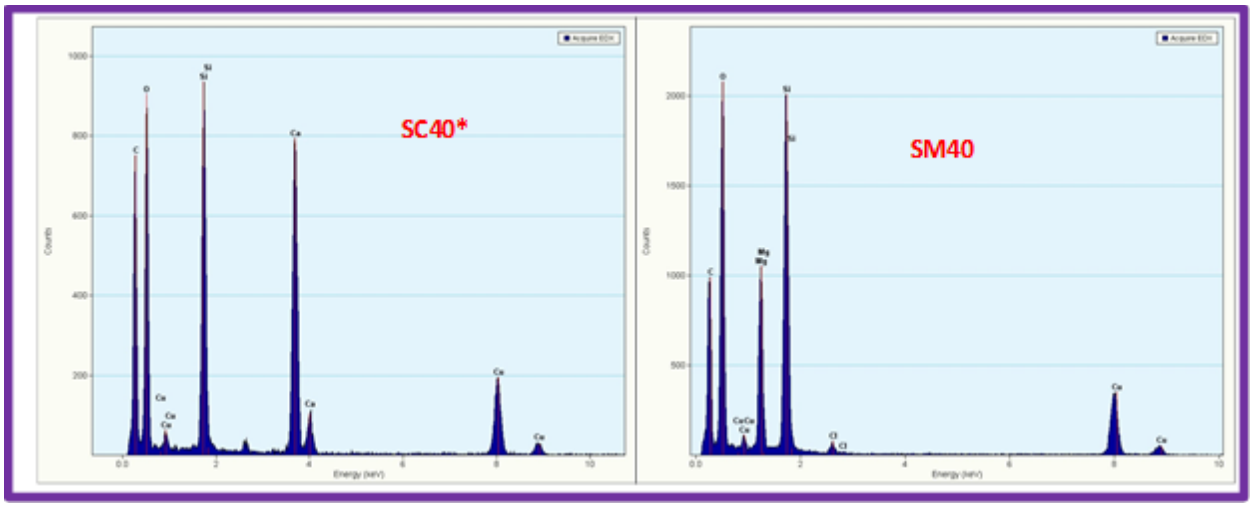

Figure S5. EDX images of the SC40*(left panel) and SM40 (right panel) samples.

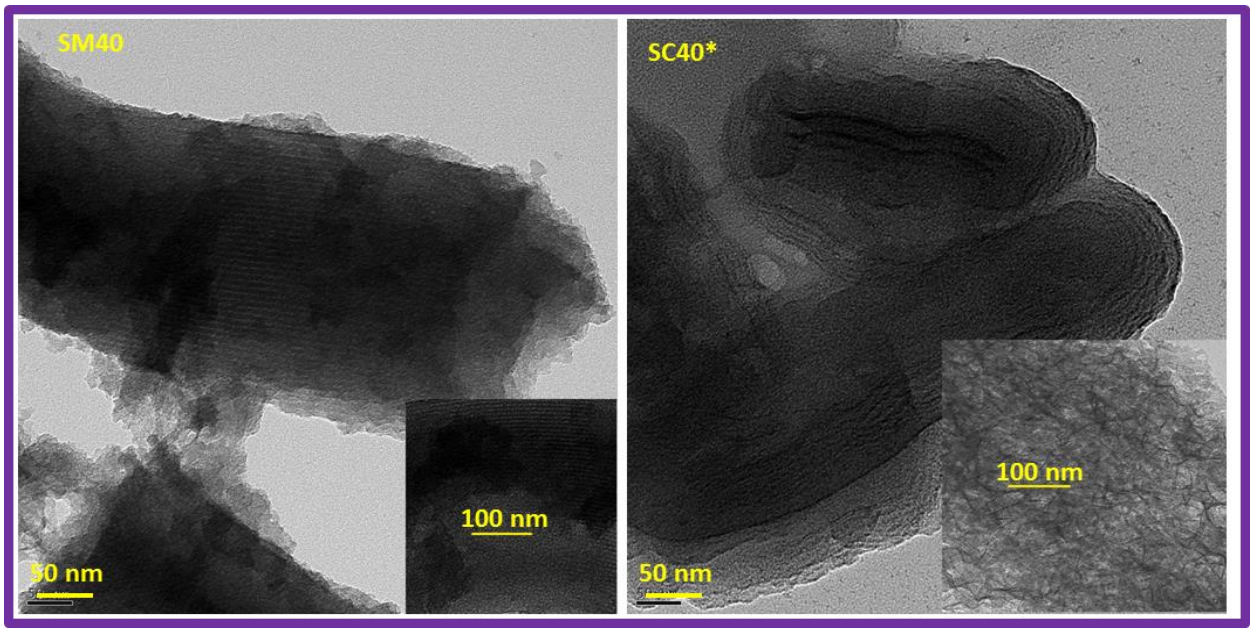

Figure S6.TEM images of the SM40 (left panel) and SC40* (right panel) samples.

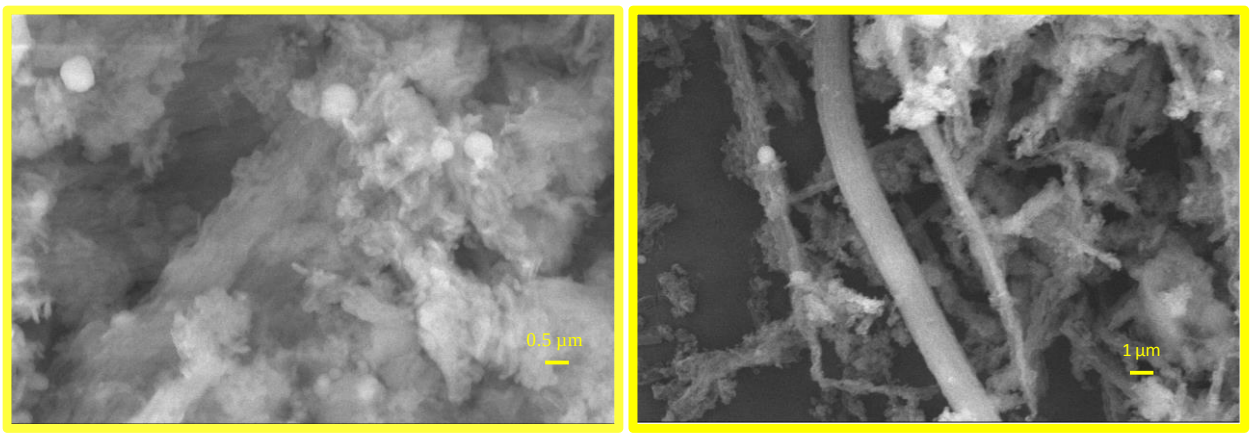

Figure S7. SEM images of the SM40 sample.

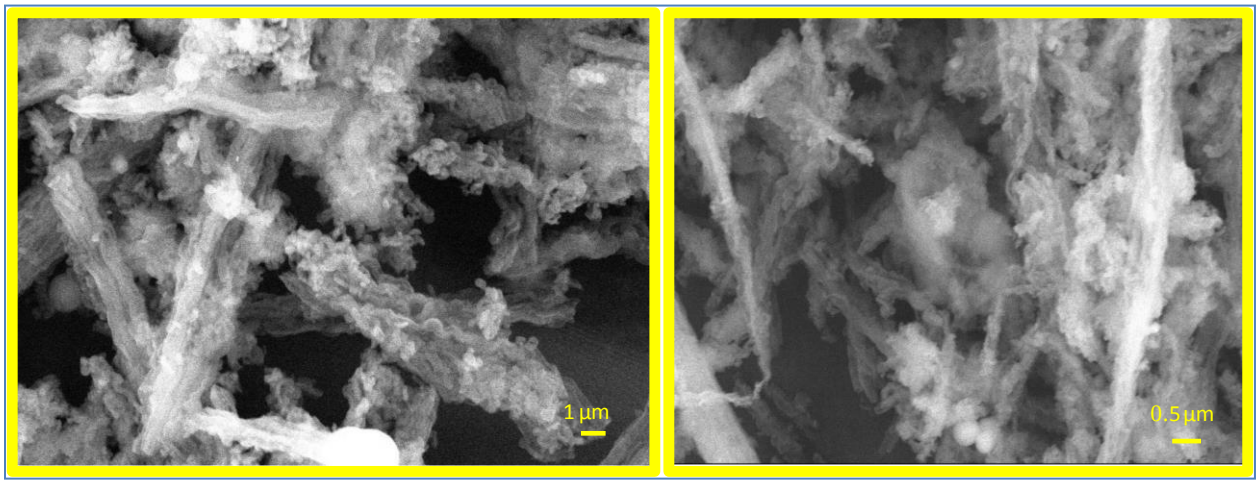

Figure S8. SEM images of the SC40* samples.

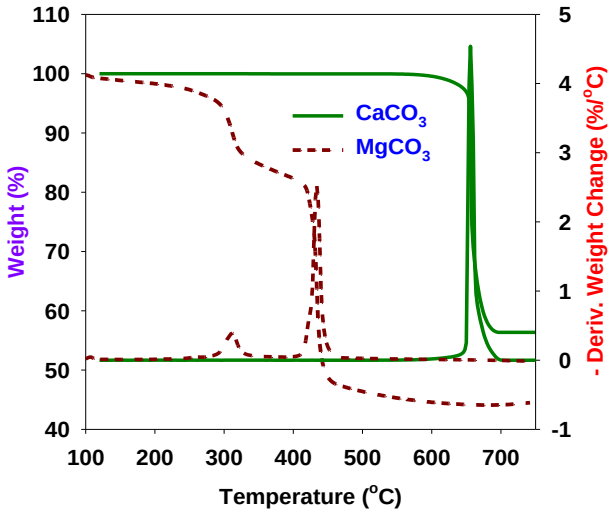

Figure S9. TG/DTG curves for commercially available $CaCO_3$ and $MgCO_3$ samples.

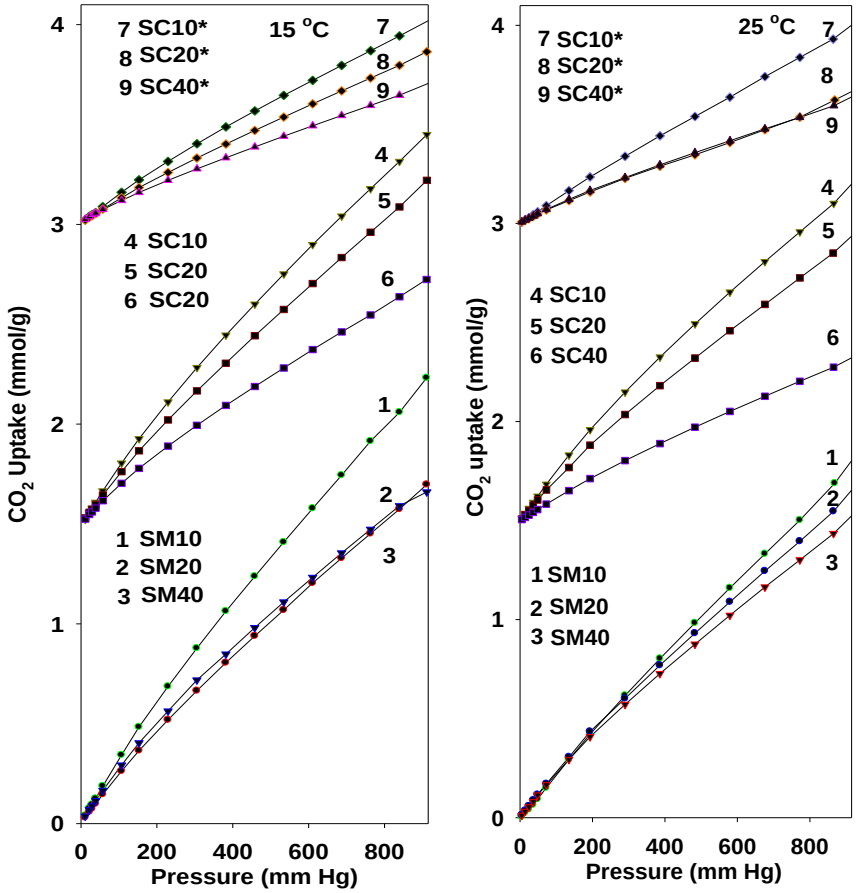

Figure S10. CO_2 adsorption isotherms at 15 °C (left panel) and 25 °C (right panel)measured on the samples studied; isotherm curves 4,5,6 and 7,8,9 are shifted by 1.5 and 3 mmol/g, respectively, in relation to curves 1,2,3.

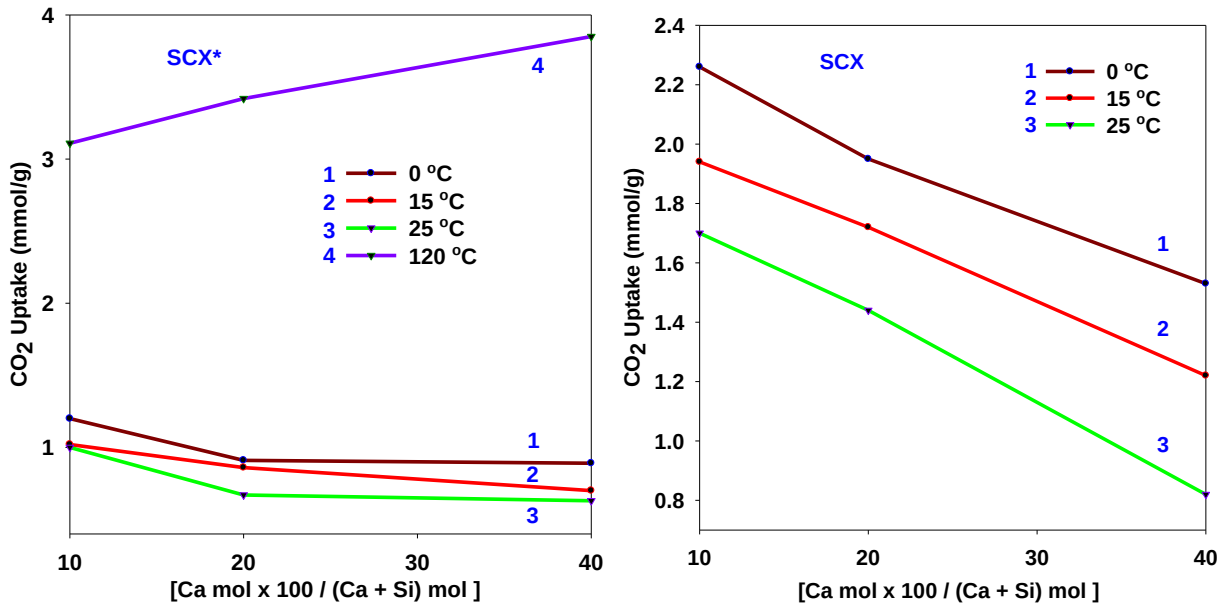

Figure S11. CO_2 uptake change with the molar percentage (X %) of Ca in the SCX* (left panel) and SCX (right panel) (X=10,20,40) composites at different temperatures.

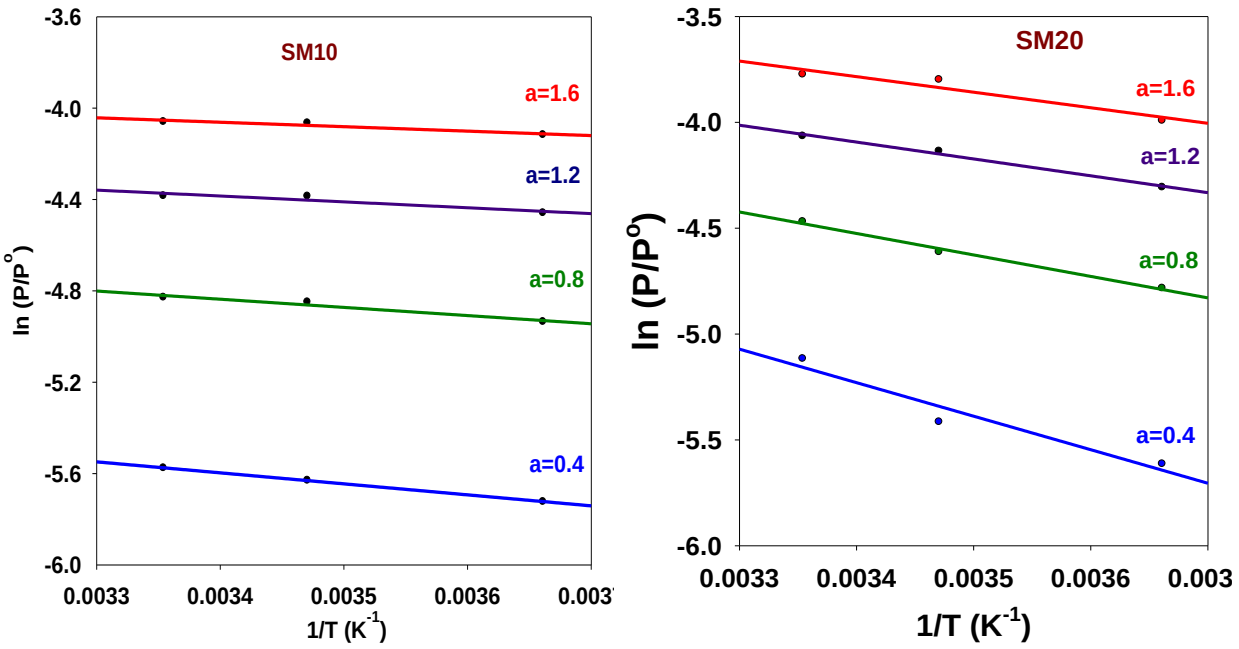

Figure S12. Variation of (lnP/P^0) with 1/T at a = 0.4, 0.8, 1.2, 1.6 mmol/g for CO_2 adsorption on SM10 (left panel) and SM20 (right panel) samples.

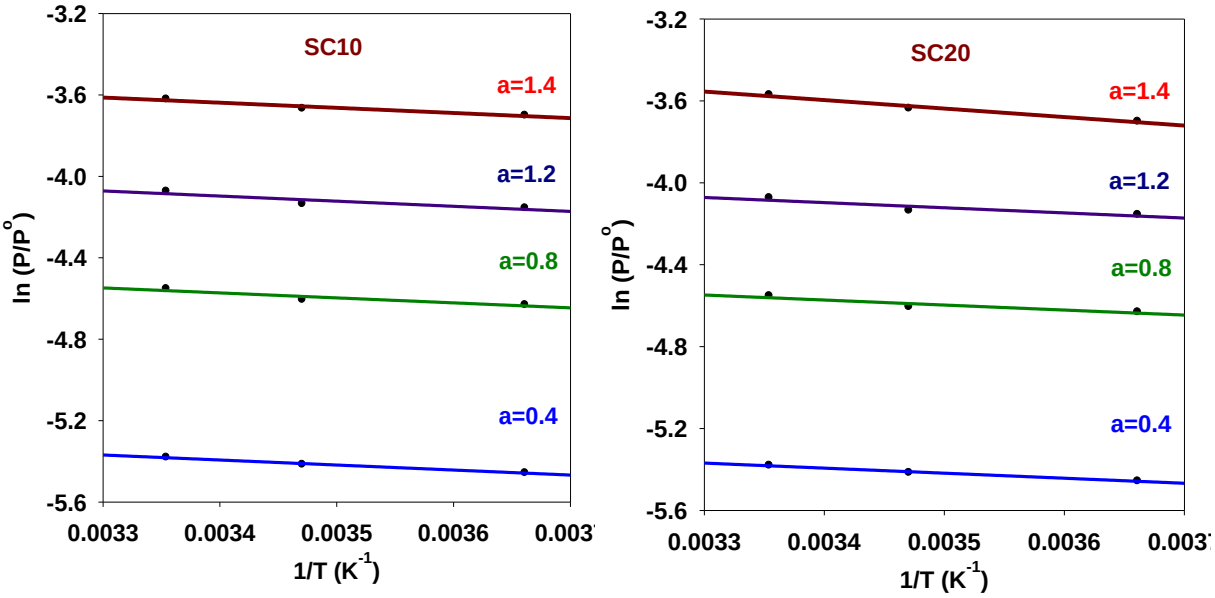

Figure S13. Variation of ($\ln P/P^0$) with 1/T at a = 0.4, 0.8, 1.2, 1.6 mmol/g for CO_2 adsorption on SC10 (left panel) and SC20 (right panel) samples.

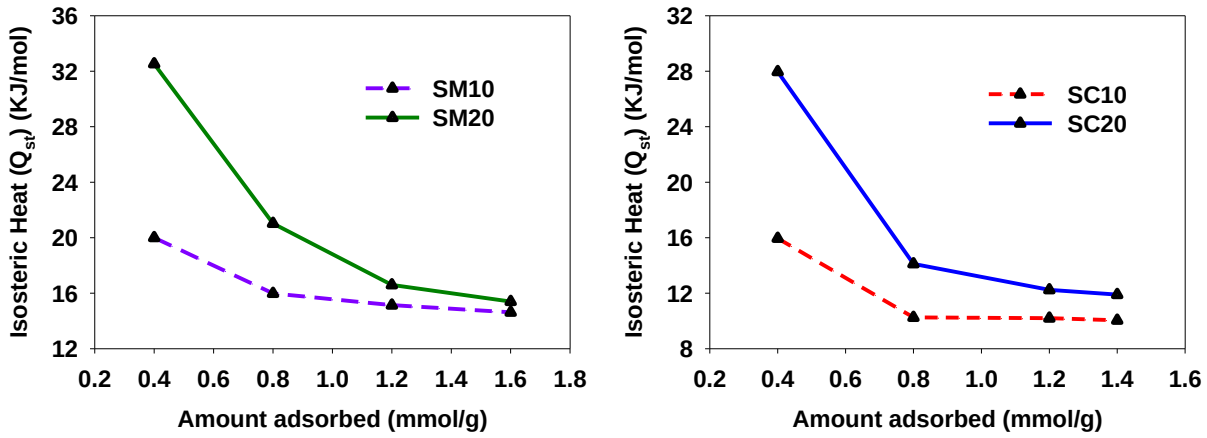

Figure S14. Variation of the isosteric heats of CO_2 adsorption for the SM10 and SM20, SC10, and SC20 samples.

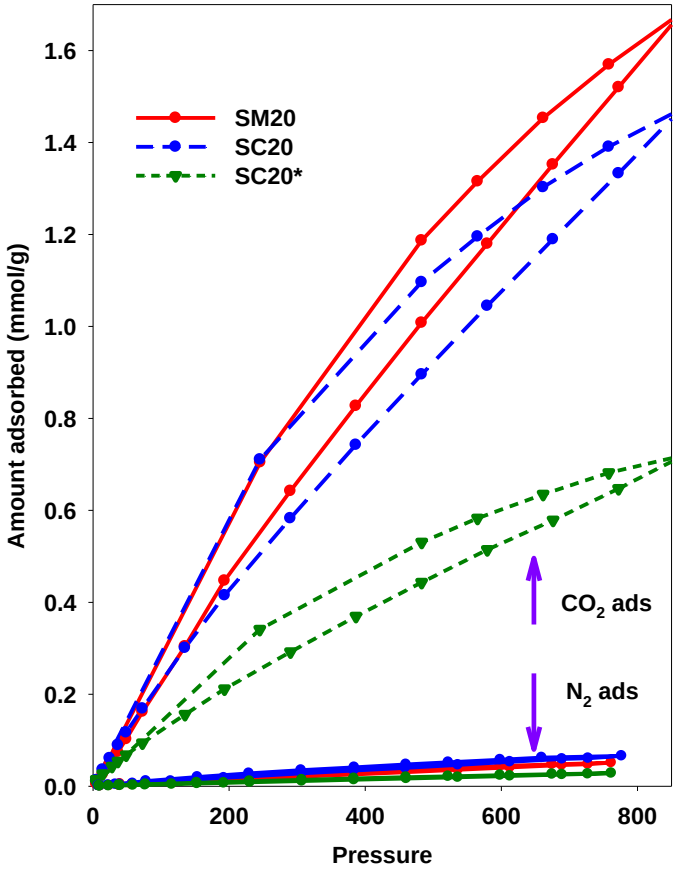

Figure S15. CO_2 and N_2 adsorption-desorption isotherms at 25 ^{o}C measured on the SM20, SC20, and SC20*samples studied.